
Liquid crystal textures and optical characterization of a dye-doped nematic for generating vector beams

^{1,2}Nastishin Yu. A., ¹Dudok T., ³Savaryn V., ¹Kostyrko M., ¹Vasylkiv Yu.,
²Hrabchak V., ²Ryzhov Ye. and ¹Vlokh R.

¹ O. G. Vlokh Institute of Physical Optics, 23 Dragomanov Street, 79005 Lviv, Ukraine

² Hetman Petro Sahaidachnyi National Army Academy, 32 Heroes of Maidan Street, 79012 Lviv, Ukraine

³ Stepan Gzhytskyi National University of Veterinary Medicine and Biotechnologies, 50 Pekarska Street, 79010 Lviv, Ukraine

Received: 29.06.2021

Abstract. In the present work, liquid-crystal (LC) textures with non-uniform director-field configurations and azimuthal singularities are considered from the viewpoint of their applications for generating vector and scalar optical vortex beams. To generate a composite vector beam, a LC sample should be light-absorbing and dichroic. For generating a scalar vortex beam, a fork-like defect should be formed in a LC cell. To assess quantitatively these possibilities, we perform optical characterization of a dye-doped nematic. Namely, we employ known characterization techniques for measuring ordinary and extraordinary light absorption indices, linear dichroism, dispersion of linear-birefringence increment, and a scalar orientational order parameter. Since a light-absorbing dopant used by us is a fluorescent dye, the vector beams can be obtained in either transmitted or fluorescent lights. For this reason, we also measure the fluorescence of our dye-doped nematic.

Keywords: vector beam, liquid crystals, dichroism

UDC: 535.34, 535.37, 544.25

1. Introduction

Nowadays the notion of liquid crystals (LCs) has become deeply rooted in our everyday life at least due to well-known liquid-crystal displays. The physical properties of LCs seem to be well understood and most of the appropriate researches are now focused on their applications. Due to orientational ordering combined with lowered dimensionality of translational ordering, LCs exhibit many unique properties. They are highly sensitive to any external fields or actions. This makes these optical materials attractive for diverse branches of natural sciences and technologies. Of course, the applied aspect of LCs prevails in these studies.

Having a lowered dimensionality (2D, 1D or 0D) of their translation order accompanied with a pronounced specific orientational order, most of the LC phases reveal optical anisotropy, quite similar to solid crystals with a true translation order. Here by ‘true translation order’ we mean that this order is three-dimensional (3D) in the solid crystals. The 3D translation order excludes fluidity, which implies that a ‘true crystal’ cannot be liquid. While columnar and smectic phases, which represent structurally respectively 2D and 1D crystals, can be called ‘LCs’, the nematic phase is not ‘crystal’ at all. It is rather a true (i.e., 3D) liquid with no translational order (i.e., with a 0D order).

Although the controversy of the term ‘LC’ is evident, it remains in use in the scientific literature, being even more popular than its more appropriate counterpart, the term ‘mesophase’. Lowered translation-order dimensionality in the LCs is caused by their fluidity in complementary

directions. In particular, the columnar, smectic and nematic phases represent respectively 2D, 1D and 0D crystals, and 1D, 2D and 3D liquids. Due to lowered dimensionality of the translation order, the optic axis (or axes) can be effectively aligned. Contrary to the solid crystals, which must be carefully grown to fabricate a uniform single crystal, uniformly aligned LCs (i.e., prototypes of solid single crystals) can be relatively easily obtained by either appropriate treatment of the bounding surfaces or application of external electric or magnetic fields.

In many cases, LC samples with a non-uniform distribution of the optic axis across a cell are needed. There are several possibilities to form a non-uniform pattern of the in-plane director distribution, including that containing defects. Special devices called spatial light modulators have been designed to control the director distribution across a nematic cell. The nematic cell in the spatial light modulator with an isolated topological defect is called as a q -plate. It is used for generating light beams carrying optical singularities. Another possibility is based on the phenomenon of photoalignment of LCs by photosensitive polymer layers coated on glass substrates, which are irradiated by linearly polarized light across a mask mimicking a desired in-plane director distribution [1, 2]. Some simple patterns, e.g. a circular director pattern, can be produced with simple mechanical rubbing. To produce a circular in-plane director distribution, one can also use a drilling machine or a hand-made device that rotates the rubbing tissue on a substrate covered with a polymer that provides planar alignment.

In this paper we focus on spatially modulated director-field configurations appearing spontaneously in LC samples. Amazing examples of such spontaneously modulated structures are fingerprint textures of cholesterics, focal conic domains in smectics, stripe textures observed when approaching nematic–smectic A (SmA) or cholesteric–SmA* phase transitions, director distributions in freely suspended drops and films, and modulated structures appearing either under competitive surface-alignment conditions or when the phase transitions are approached. To generate a vector light beam of light, the LC sample should be absorbing and linearly dichroic [3]. To assess quantitatively such a possibility, we perform optical characterization of a dye-doped nematic. Namely, we employ a standard optical characterization technique [4, 5] to measure the ordinary and extraordinary absorption indices, the linear dichroism, the dispersion of linear optical-birefringence increment, and the scalar orientational order parameter. Since our absorbing dopant is a fluorescent dye, the vector beams can be obtained in either transmitted or fluorescent lights. Therefore we measure the fluorescence of our dye-doped nematic.

2. LC textures for generating vector beams

For the sake of clarity, we recall that the light vortex beam (VB) is a perfectly polarized beam for which the polarization state is a function of the in-plane coordinates. Here and further throughout the text, the term ‘in-plane’ refers to the cross-section normal to the beam axis. A special class of VBs is a vector VB (VVB) that carries polarization singularity. It is understood that the intensity of the VB exiting a polarizer is a function of in-plane coordinates, which varies when the polarizer is rotated. The light intensity for the VVB is zero at the coordinates that correspond to beam singularity.

Two principally different approaches, or so-called *direct* and *indirect* techniques, are used for generating the VBs. Lasers with specially designed resonators are used for the direct generation [6–8], whereas specially designed singular optical elements are needed to transform a beam from the conventional laser into the VVB [9–13]. A key component of any singular optical element is topological singularity/singularities available in the in-plane distribution of the optic axis.

Interestingly, any LC defect disturbing the director field on the scales larger than the light wavelength represents such a singularity. Therefore, the LC disclinations which, by definition, are singularities of the director field can be used for generating the VVBs. It is the advantage of LCs that the disclinations can appear even if no special attempts have been made to produce them. However, defective samples with uncontrolled director distributions, which usually appear in many LC cells with untreated substrates, are of low interest because their behaviour is hardly predictable, in both reconstruction of the director field and its reproduction. The problem is that anchoring of LC molecules on a solid substrate is governed by the surface profile on micro-scales, which is random and so hardly predictable for any untreated surface.

The situation is essentially improved if the LC sample is placed on a surface of isotropic liquid, which is immiscible with the LC. Hydrophilic liquids such as, e.g., water, glycerol, ethylene glycol are immiscible with the thermotropic LCs (which are hydrophobic) and provide planar alignment for the LC molecules on their surfaces [14]. At the opposite interface with air, the LC molecules align perpendicularly to the interface (homeotropic orientation). As a result, we have competitive (*hybrid*) anchoring at the opposite surfaces that depends on the thickness of LC film. The director field is planar if the film is thinner than the so-called anchoring extrapolation length $\xi_{l-LC} = W_{l-LC}/K_1$ (with the index $l-LC$ referring to the interface of LC with isotropic liquid (l), W_{l-LC} being the anchoring-strength coefficient, and K_1 denoting the elastic modulus for the splay deformation of director).

For thicker LC films, with the thicknesses $d > \xi_{l-LC}$, the director orientation varies across the film thickness from planar at the $l-LC$ interface to homeotropic at the interface with air. It is worth recalling that the $l-LC$ interface aligns the director parallel to it, thus fixing the zenithal angle (i.e., the angle between the director and the interface normal) at $\theta = 90^\circ$. On the other hand, the azimuthal angle φ (i.e., the angle in the plane of interface) is degenerate, since no specific direction is set by the isotropic liquid. The term ‘degenerate planar alignment’ implies that any φ value is allowed if the in-plane director distribution is uniform. It turns out that, for the hybrid-aligned LC films thicker than ξ_{l-LC} , the actual director distribution in the planes parallel to film interfaces is not uniform, being different for different LC phases.

Nematic, SmA and cholesteric LCs placed on isotropic liquids show a great variety of textures visualized easily with polarization-optical microscopy. Namely, one observes stripe domains, lattices of defects, non-trivial and high-strength defects and sessile drops with isolated defects [15, 16] in the nematics. For the SmA films one can mention the textures of so-called oily streaks and closely packed elliptic or parabolic focal conic domains (FCDs). Finally, we have parabolic FCD textures also in the cholesterics. Below, we suggest employing those structures as singular optical elements for generating the VVBs. After doping the LC materials with dichroic dyes, one can obtain a coordinate-dependent in-plane distribution of the light intensity even with no analyzer available in the optical scheme.

2.1. Singular structures in nematic films

It is obvious that, for the nematic film with hybrid alignment, the gradient of director orientation over the film thickness d increases with decreasing d , diverging to infinity at $d \rightarrow 0$. This means that the energy of elastic deformation should also diverge at $d \rightarrow 0$ for the hybrid-aligned nematic film. As a result, a smooth change of the director orientation in real samples takes place only for thick enough films, with the thicknesses $d \geq 10 \mu\text{m}$. On the other hand, the director distribution across the film thickness is homogeneously planar for thinner films (i.e., at $d < \xi_{l-LC}$).

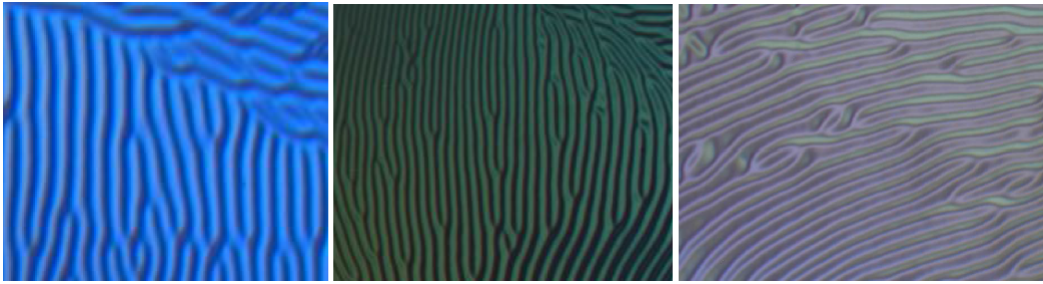


Fig. 1. Stripe domains in a hybrid nematic film placed on ethylene glycol. Numerous fork-like defects are observed, which are dislocations in the field of stripes.

For thermotropic nematics typically $\xi_{l-LC} \sim 1 \mu\text{m}$. For the intermediate thicknesses of the order of a few microns, one observes spontaneous formation of modulated and defect-involving structures, which can self-organize into periodical patterns. Theoretical considerations [12, 13] show that the energy of some defective configurations in such a film can become negative, i.e. the total elastic energy of the hybrid-oriented defective film is less than that of the smoothly deformed film. The experimental observations testify that the defects in such films can spontaneously self-organize into the structures with translational ordering, thus forming 2D lattices. The stripe textures shown in Fig. 1 illustrate some examples of spontaneously modulated director-field configuration in these thin nematic films. The dislocations in the periodical stripe textures clearly seen in Fig. 1 can be used as the singularities generating VBs.

In Ref. [17], a stripe texture has been formed in a light-transparent cholesteric cell under homeotropic-anchoring conditions in the external magnetic field. It has been demonstrated to be capable of generating the VBs. Despite the difference in the origin and exact director configuration, both stripe textures with dislocations (those presented in [17] and shown here in Fig. 1) can be used for generation of VB with the dye added to the LC material.

The other types of the defect structures appearing in thin nematic films on the surfaces of isotropic liquids, which can also be used for generating the VVBs, have been introduced in Refs. [14, 15]. A dye can be added to the LC material to achieve this goal. Different textures are observed, depending on the film thickness. The latter can be adjusted by the amount of LC material placed on the surface of the liquid. At high enough amounts, a sessile drop similar to that shown in Fig. 2 can coexist with the thin film. Then a disclination with the topological strength +1 and a characteristic texture of four extinction brushes is clearly seen. When doping nematic materials with dyes, one can use the defect in such a sessile droplet for generating the VVBs.

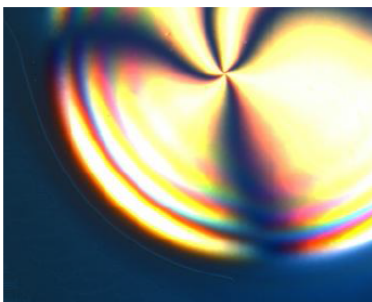


Fig. 2. A sessile nematic drop on a liquid substrate.

One can mention that liquid substrates are somewhat inconvenient for practical applications. Nevertheless, one has to take into account that, at present, the reliable alignment techniques producing degenerate hybrid-alignment conditions are in great demand. Then a scheme that

involves a LC film on an isotropic liquid is still acceptable at least for the fundamental studies. Moreover, it could be applied as a singular optical element for VVB generation. It is also worth noting that an attempt at obtaining the degenerate hybrid alignment with a solid substrate has been reported in Ref. [18] for a particular case of glass substrate wetted with glycerol. In the latter approach, a clean glass substrate was wiped with a napkin wetted with glycerol. The LC film was prepared by spreading a nematic material with a blade over the glycerol-wetted substrate. In Fig. 3 we show a so-called Shlieren texture observed for a nematic E7 film (from Merck) spread over a glycerol-wetted glass substrate. Defects with a half-integer topological strength of $\frac{1}{2}$ and two extinction brushes outgoing from the cores of defects are seen in Fig. 3.

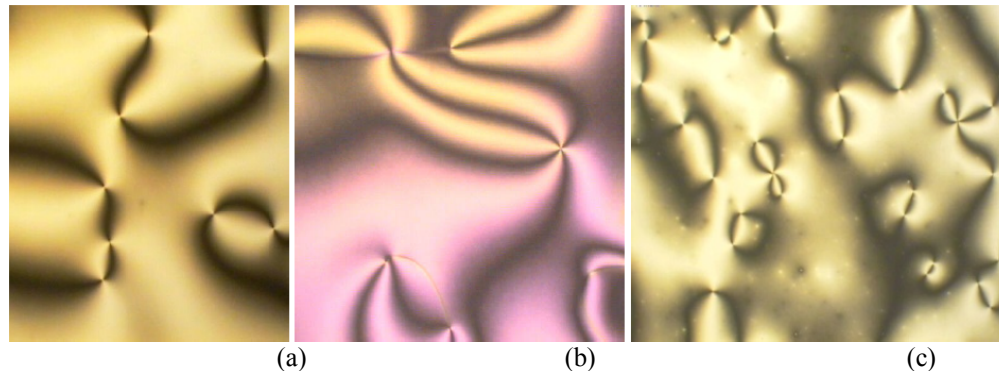


Fig. 3. Shlieren textures observed in a nematic E7 film placed on a glycerol-wetted glass substrate. Panels (a) and (b) correspond respectively to the room temperature and the temperature $T = 55.4^\circ\text{C}$ close to the transition into isotropic phase.

It is worth recalling that the topological strength of disclination in nematics can be calculated as $|s| = N/4$, where N stands for the number of extinction brushes outgoing from the defect core. For all the eight defects observed in Fig. 3a, one finds $N = 2$ and so we have $|s| = 2/4 = 1/2$. There is a single defect in Fig. 3b and two defects with four extinction brushes in Fig. 3c. In the latter case we have $N = 4$ and, hence, all the topological strengths are equal to $|s| = 4/4 = 1$.

It is important that, at the room temperature (i.e., far from the nematic–isotropic phase transition), the defects with the half-integer strengths in Fig. 3a are isolated, so that no other defects are attached to their cores. This indicates that the alignment observed at the nematic–isotropic liquid interface is strictly planar (i.e., nematic molecules are exactly parallel to the interface). On the contrary, thin bright lines attached to the defects with the half-integer strengths in Fig. 3b, which represent defect walls, point to the fact that the nematic director becomes tilted with respect to the nematic–isotropic liquid interface in the vicinity of the nematic–isotropic transition. By the topological requirements, the defect walls should be attached rather to the defects with half-integer strengths (with the two extinction brushes) than the integer-strength defects (with the four extinction brushes). This is indeed seen from Fig. 3b.

The dye-doped nematic samples with the Shlieren textures such as those observed in Fig. 3 can be used as singular optical elements for generating VVBs. In the next section, we will discuss the SmA films under degenerate hybrid-alignment conditions prepared with the same alignment techniques.

2.2. Singular SmA films

Out of doubt, the FCDs in smectics are the most prominent among the LC defects. They have been remaining maybe one of the most impressive objects in the physics of condensed matter for more

than a century. Two types of the FCDs can be observed in smectics, elliptical and parabolic ones. In the elliptical (or parabolic) FCDs, equidistant parallel smectic layers are folded around a pair of singularities, respectively a confocal ellipse or a hyperbola (two parabolas). In a special case, the ellipse and the hyperbola of the elliptical FCD can reduce to respectively a circle and a straight line passing through the centre of this circle [19]. In an ideal elliptical FCD, equidistant smectic layers form a family of parallel surfaces, so-called Dupin cyclides. The parabolic FCDs can be observed in the cells with planar alignment or in the homeotropic cells under the strain available along the cell normal. The elliptical FCDs can be obtained in the thick cells with untreated glass substrates after melting from the solid state to the SmA phase. A hexagonally packed system of elliptic FCDs can be obtained in the SmA samples under hybrid-anchoring conditions. We recall that the latter conditions imply homeotropic alignment of the director at one interface of the smectic film and planar alignment at the opposite interface.

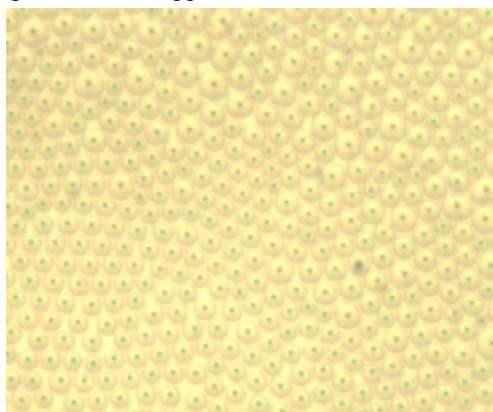


Fig. 4. Polarization-optical microscopy texture of SmA film on the surface of glycerol without an analyzer.

The hybrid alignment of SmA can be obtained in the flat cell assembled from two glass substrates providing respectively homeotropic and planar alignments. An alternative scheme is a thin film deposited on an isotropic hydrophilic liquid (glycerol, water, ethylene glycol, etc). In the latter case, the planar director alignment at the interface of SmA with the isotropic liquid is degenerate, since no direction is specified by the isotropic liquid.

The alternative bounding anchoring conditions imposed on the zenithal angle of the director imply a curvature of the director field along the film thickness which, in its turn, imposes some curvature of the smectic layers. Smooth variation of the director from the planar orientation to the homeotropic one would produce splay and bending deformations of the director field. The bend deformation of the director implies a splay deformation of the smectic layers, which strongly violates equidistance and parallelism of the smectic layers and, thus, is forbidden in smectics. As a result, the structure of thick enough ($d > 10 \mu\text{m}$) hybrid-aligned SmA films splits into a quasi-hexagonally packed system of elliptic FCDs (Fig. 4), for which the ellipses are transformed into circles and hyperbolas into straight lines. The plane of the circles is parallel to the film surfaces, i.e. parallel to the observation field, while the straight line is oriented along the normal to the film plane, being normal to the observation field. Dark dots in the centres of the circles are projections of the straight-line disclinations in the field of microscope. The diameters of the circles are comparable to the thickness of the film. In the crossed polarizers, this texture is composed of a quasi-hexagonal array of Maltese crosses (Fig. 5).

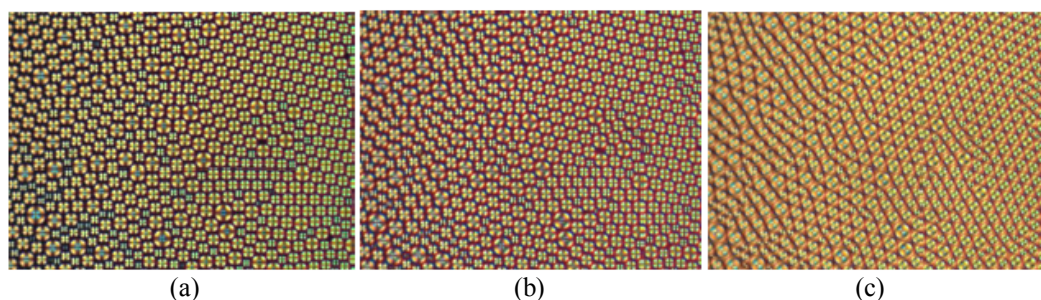


Fig. 5. A quasi-hexagonally ordered structure composed of FCDs is observed in the case of SmA film placed on a glycerol surface. Panel (a) corresponds to observation in crossed polarizers and panels (b) and (c) respectively to additional λ plate and $\lambda/4$ plate inserted before the analyzer.

Similarly to the case of nematic films addressed above, the hybrid-aligned smectic films can be prepared when depositing a smectic material onto a glycerol-wetted substrate (see Fig. 6). In this case, the FCDs appear to be fragmented and distorted by kinks on the ellipses. For thick enough films, one can find kinked FCDs such as those observed with optical microscope (see Fig. 7).

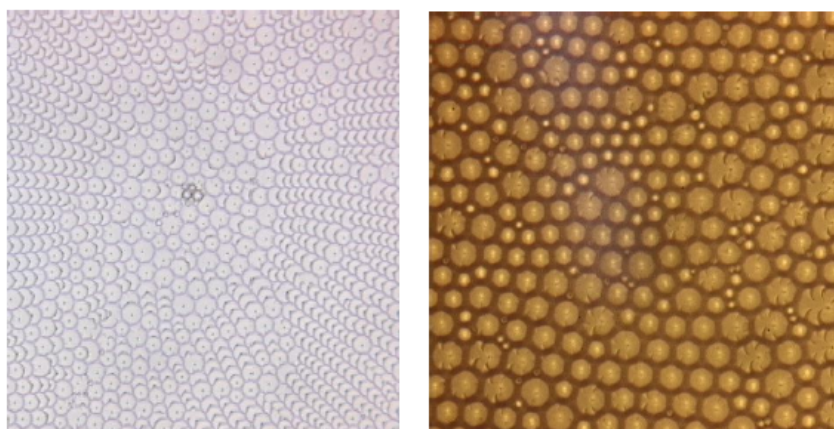


Fig. 6. System of fragmented and kinked FCDs, as observed with no polarizers in the SmA film placed on a glycerol-wetted substrate.

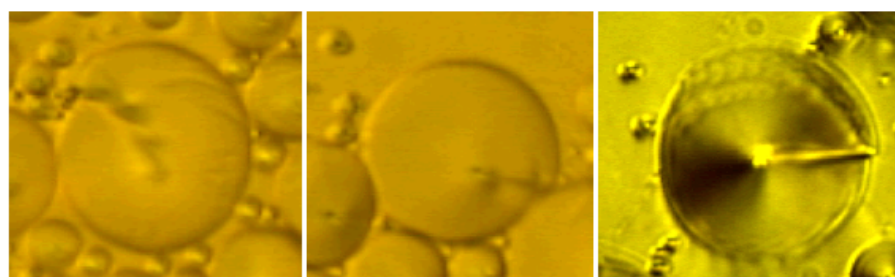


Fig. 7. Kinked FCDs observed with optical microscope for the SmA film deposited on glycerol-wetted substrates.

In the cells assembled of the glass substrate covered with the layers for the planar and homeotropic alignments, the SmA sample splits into a quasi-hexagonal array of domains as shown in Fig. 8. Finally, in the cells with the glass substrates covered by rubbed polymers for the planar alignment, one finds a system of parabolic domains (see Fig. 9).



Fig. 8. Quasi-hexagonal array of domains observed under polarization microscope (with no analyzer) in a SmA cell with hybrid alignment.

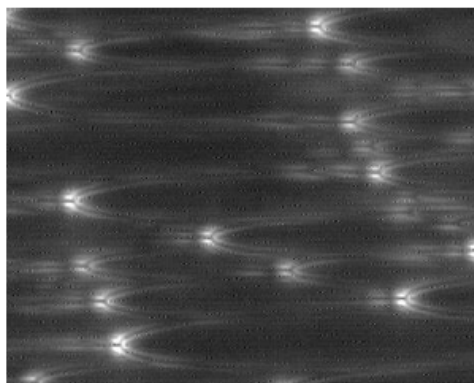


Fig. 9. A system of parabolic FCDs observed in a planar smectic cell.

A laser beam directed at the dye-doped structures as those shown in Fig. 4, Fig. 5, Fig. 6 and Fig. 8 should diffract and form a system of VBs. The kinked FCDs (see Fig. 7) appearing in the dye-doped SmA films deposited on the glycerol-wetted substrates can also be used for generating VBs. Moreover, the parabolic FCDs shown in Fig. 9 are worthwhile for this aim, too.

2.3. Self-organized structures of defects in cholesterics

In addition to the nematic and smectic LC phases where the director in the ground state is homogeneous, there are the LC phases with spontaneously modulated structures of the field director. An example is the cholesteric phase. In its ground state, the director twists spontaneously around the axis which is at each point perpendicular to the director such that the azimuthal angle of the latter is a continuous function of the coordinate along the axis of twist. The distance measured along this axis at which the director rotates by 360° is called a pitch (P) of the cholesteric twist.

The elastic properties of short-pitch cholesterics are similar to those of the smectics. Therefore the corresponding polarization-microscopic textures in some cases resemble the smectic textures. Here the cholesteric pitch plays a role of interlayer distance. In particular, we have also a regime of equidistance and parallelism of cholesteric layers, which is achieved through the formation of parabolic FCDs.

Similar to the smectics, a thin film of short-pitch cholesteric with degenerate hybrid boundary conditions, which is placed on a glycerol surface, also splits into domains. The typical appropriate textures contain the oily streaks composed of parabolic FCDs (see Fig. 10).

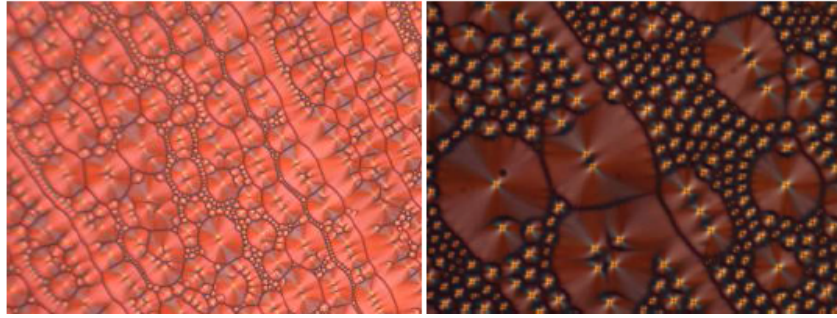


Fig. 10. Polarization-optical microscopy textures observed in a cholesterol film placed on a glycerol surface.

The defect structures observed in the dye-doped cholesterics placed on the glycerol-wetted substrates (see Fig. 11) also seem to be promising for the generation of VVBs.

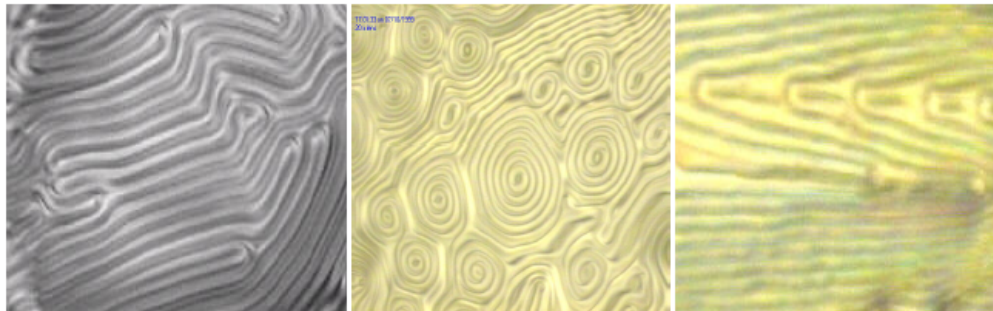


Fig. 11. Textures observed in a cholesteric film placed on a glycerol-wetted substrate.

3. Optical characterization of a dye-doped nematic

Conventional thermotropic LCs, including nematics, smectics and cholesterics, are transparent for the visible light. In the case of absorption present, any optically anisotropic material has to manifest some dichroism. A polarized light beam passing through such a sample with azimuthally singular distribution of the director would have become a VVB [3]. Dichroism of the conventional thermotropic LCs can be obtained by doping them with some guest dye molecules, which can be pre-aligned by the hosting LC matrix.

We prepared a mixture of optically transparent nematic E3100-100 (from Merck) with 0.8 wt. % of fluorescent dye Nile Red. To perform optical characterization of this dichroic nematic material, we placed it into a cell (with the thickness $16.7\mu\text{m}$) assembled of the glass substrates covered with a mechanically rubbed polyimide PI-2555 alignment layer. The latter provided unidirectional planar alignment of the director along the rubbing direction. Then we used the geometry of parallel polarizers and measured the light transmissions T_0 , T_{45} and T_{90} , which refer respectively to the azimuthal orientations 0° , 45° and 90° of polarizers with respect to the director.

3.1. Absorption indices and dichroism

In the framework of optical characterization technique [1, 2], the absorption indices along the director (κ_{\parallel}) and perpendicular to it (κ_{\perp}) and the dichroism $\Delta\kappa = \kappa_{\perp} - \kappa_{\parallel}$ are calculated as

$$\kappa_{\parallel} = -\frac{\lambda}{4\pi d} \ln T_0, \quad \kappa_{\perp} = -\frac{\lambda}{4\pi d} \ln T_{90}, \quad \Delta\kappa = \frac{\lambda}{4\pi d} \ln \frac{T_{90}}{T_0}, \quad (1)$$

where λ is the light wavelength and $d = 16.7 \mu\text{m}$ the thickness of our nematic sample. For a plate with a given thickness d , it is convenient to introduce a so-called relative dichroism σ :

$$\sigma = \exp(-2\pi d \Delta\kappa / \lambda). \quad (2)$$

It is seen from Eq. (2) that one has $\sigma = 1$ in the absence of dichroism ($\Delta\kappa = 0$) and $\sigma \rightarrow 0$ in the case of infinitely large dichroism ($\Delta\kappa \rightarrow \infty$). The experimental $T_0(\lambda)$, $T_{90}(\lambda)$ and $T_{\pm 45}(\lambda)$ dependences are shown in Fig. 12, whereas the calculated spectral dependences of the $\Delta\kappa$ and σ parameters are presented in Fig. 13.

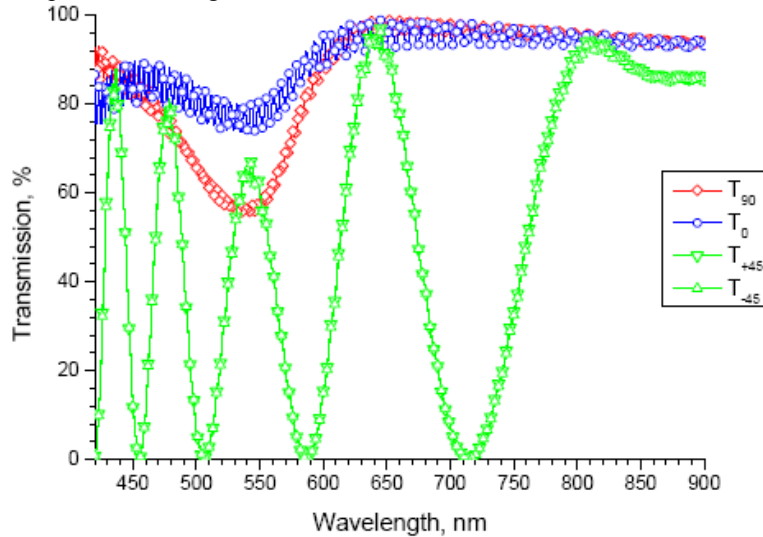


Fig. 12. Experimental spectral dependences $T_0(\lambda)$ (circles), $T_{90}(\lambda)$ (diamonds) and $T_{\pm 45}(\lambda)$ (triangles).

One can see from Fig. 12 that the minimal transmissions $T_0(\lambda)$ and $T_{90}(\lambda)$ for the dye suspended in the LC matrix correspond to the light wavelength ~ 550 nm. This corresponds to the centre of the absorption band stretched from 450 to 650 nm. The transmission dependences $T_{\pm 45}(\lambda)$ oscillate with the varying wavelength due to refraction anisotropy. From these dependences, one can calculate the orientational scalar order parameter of the dye molecules:

$$S = \frac{n_{\parallel} \ln T_0 - n_{\perp} \ln T_{90}}{n_{\parallel} \ln T_0 + 2n_{\perp} \ln T_{90}}, \quad (3)$$

where the refractive indices measured parallel and perpendicular to the director for our nematic are respectively equal to $n_{\parallel} = 1.72$ and $n_{\perp} = 1.57$. The order parameter calculated from the data of Fig. 12 is equal to -0.23 .

The maximal difference in the absorptions for the orthogonal eigenpolarizations of light is also reached at ~ 550 nm (see Fig. 12). Hence, this wavelength corresponds to the maximal dichroism, too (see Fig. 13a). However, the dichroism is not so high. The parameter σ drops down from the maximal unit value only to $\sigma = 0.86$ at the maximal-absorption wavelength ~ 550 nm (see Fig. 13b). This gives the absorption difference for the orthogonal eigenpolarizations as small as 14%.

The latter fact implies the following: when a q -plate is constructed using such a dichroic LC matrix and the incident light is circularly polarized, the emerging beam would become a VVB. Then the polarization would become elliptical but not linear, with some radial (azimuthal) distribution. The

eccentricity of the polarization ellipse would be equal to 0.31. Note that, if $0 < \sigma < 1$, a composite VVB appears, with the incorporated beams having the orbital angular momenta $2q$ and q , and the polarization order equal to q [3] (q - is the strength of topological defect).

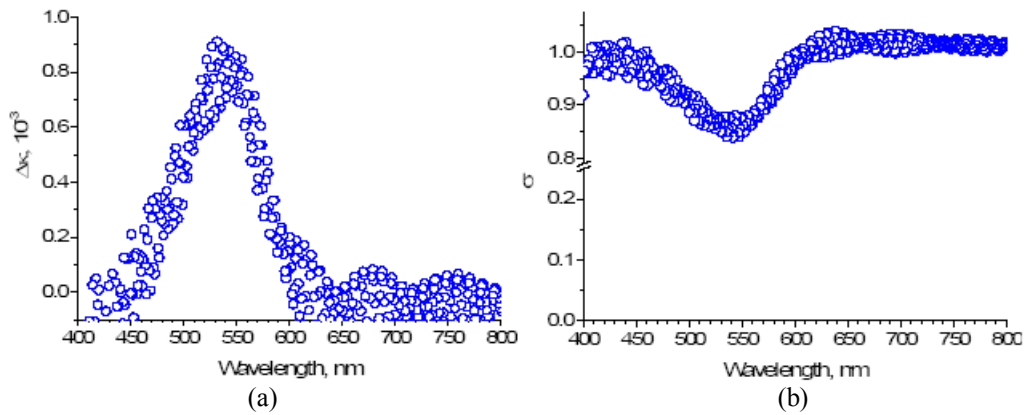


Fig. 13. Calculated spectral dependences of $\Delta\kappa$ (a) and σ (b) parameters.

3.2. Dispersion of linear birefringence

Using the spectral T_0 , T_{45} and T_{90} data and the expression

$$\cos\Delta\Phi = \frac{4T_{45} - (T_0 + T_{90})}{2\sqrt{T_0 T_{90}}}, \quad (4)$$

we have calculated the increment of phase retardation and the dispersion of the birefringence increment $\delta(\Delta n) = \frac{\lambda}{2\pi d} \Delta\Phi$, which is equal to the true birefringence up to a constant factor.

Following from the absolute birefringence value (0.15) known at 632.8 nm, we have obtained the final dispersion dependence for the absolute magnitude of linear birefringence. The dispersion of the parameters $\cos\Delta\Phi$, $\delta(\Delta n)$ and Δn are shown in Fig. 14. As seen from Fig. 14, the dispersion of the birefringence has a normal character, in spite of the weak absorption band available in the spectral region under study.

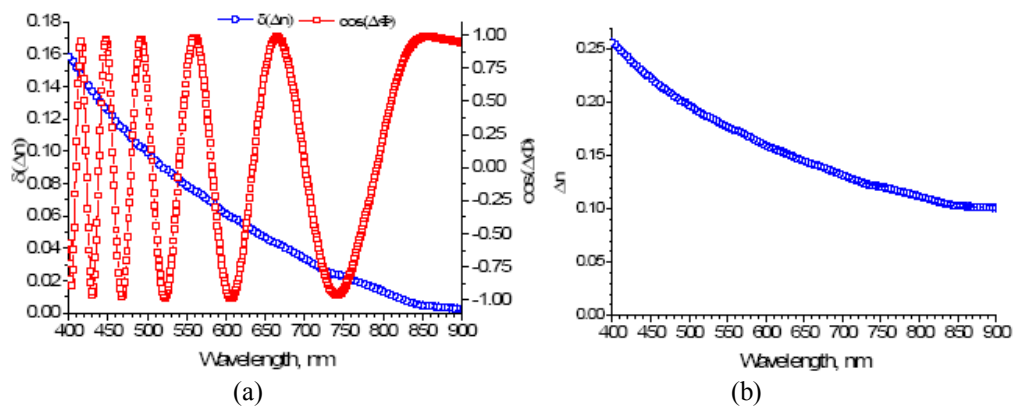


Fig. 14. Dispersions of $\cos\Delta\Phi$ parameter and birefringence increment (a), and dispersion of birefringence (b), as obtained for our dye-doped nematic.

3.3. Fluorescence

The experimental set-up used for measuring the fluorescent response of our dye-doped nematic cell is shown in Fig. 15. The intensity of fluorescent light of a DPSS laser with the wavelength $\lambda = 532$ nm is shown in Fig. 16. Notice that the fluorescence intensities referred to different spectral curves in Fig. 16 cannot be directly compared with each other, since all of the four curves correspond to somewhat different experimental procedures. Nonetheless, we are confident that, when the linearly polarized light excites our sample, the fluorescence radiation should be elliptically polarized, since the two orthogonal components reveal different intensities. When the polarizations of the exciting radiation and the fluorescence are perpendicular to the director, the fluorescence intensity is higher than that detected for the other cases. On the other hand, the intensity of fluorescence radiation polarized parallel to the director is not much smaller for the same orientation of polarization of the exciting radiation. Under conditions when the radiation is transferred between orthogonal polarizations of excitation and fluorescence radiation (full circles and triangles in Fig. 16), the fluorescence intensity differs sufficiently for orthogonal polarizations. However the intensity of fluorescence for orthogonal polarizations for the case of parallel polarizations of excited and fluorescence radiation is quite close (open circles and triangles in Fig. 16). It means that, in principle, in the both cases elliptically polarized fluorescence emerges from the sample, however, the eccentricity of the ellipse of polarization is higher in the first case.

These facts suggest that, in principle, one can expect the appearance of the VBs in the fluorescence radiation whenever the appropriate polarization distributions of exciting radiation are provided.

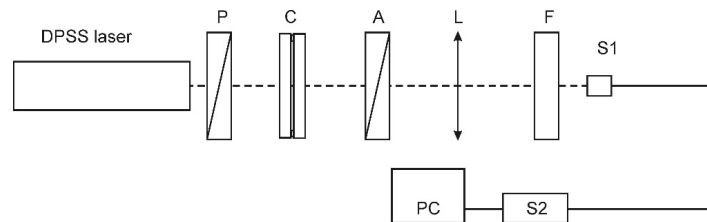


Fig. 15. A scheme of experimental set-up employed for fluorescence measurements: P – polarizer, C – dye-doped nematic cell under test, A – analyzer with angle-reading device, L – focusing lens, F – filter that removes the light of excitation laser, S1 – optical adapter of fibre spectrometer S2 (Avantes_USB_2021), and PC – controlling personal computer.

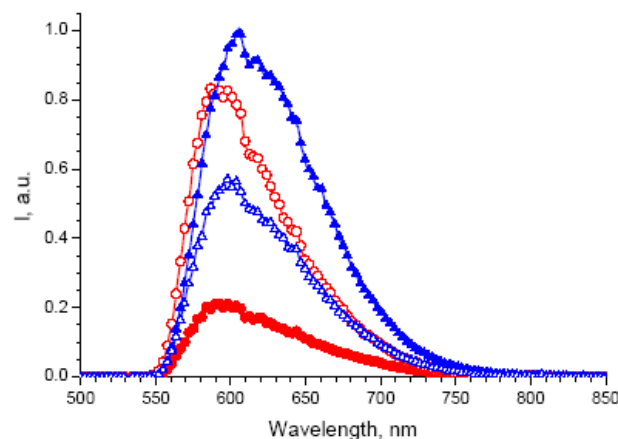


Fig. 16. Fluorescence of our dye-doped nematic excited with DPSS laser (the wavelength $\lambda = 532$ nm). The polarization of exciting radiation is parallel (circles) or perpendicular (triangles) to the director. Open circles and triangles correspond to the fluorescence polarization parallel to that of the exciting radiation, while full circles and triangles to the fluorescence polarization perpendicular to that of the exciting radiation.

4. Conclusions

In the present work, we have systematically described various LC textures that manifest non-uniform director-field configurations and azimuthal singularities. A number of amazing examples of such spontaneously modulated structures have been demonstrated: the fingerprint textures in cholesterics, the FCDs in smectics, the stripe textures observed if one approaches the phase transitions nematic–SmA and cholesteric–SmA*, the director distributions observed in freely suspended LC films, and the modulated structures appearing under competitive surface-alignment conditions or when approaching the phase transition points.

To generate a composite VB, the LC sample should be optically absorbing and dichroic. To address quantitatively this situation, we have characterized optically a dye-doped nematic LC. Namely, we have employed the characterization technique [1] in order to measure the ordinary and extraordinary absorption indices, the linear dichroism, the linear birefringence and the scalar orientational order parameter. Since the light-absorbing dopant used by us is a fluorescent dye, the VBs can be obtained in either transmitted or fluorescent lights. Finally, we have measured the fluorescence of our dye-doped nematic LC and obtained its quantitative characteristics.

References

1. Yaroshchuk O and Reznikov Y, 2012. Photoalignment of liquid crystals: basics and current trends. *J. Mater. Chem.* **22**: 286–300.
2. Yubing Guo, Miao Jiang, Chenhui Peng, Kai Sun, Yaroshchuk O, Lavrentovich O D and Qihuo Wei, 2017. Designs of plasmonic metamasks for photopatterning molecular orientations in liquid crystals. *Crystals*. **7**: 8.
3. Kostyrko M, Krupych O, Vasylykiv Y, Skab I and Vlokh R, 2021. Topological defects related to linear dichroism. Generation of vector-vortex beams. *Optik*. **230**: 166335.
4. Nastishin Yu A, Liu H, Schneider T, Nazarenko V, Vasyuta R, Shiyonovskii S V and Lavrentovich O D, 2005. Optical characterization of the nematic lyotropic chromonic liquid crystals: light absorption, birefringence, and scalar order parameter. *Phys. Rev. E*. **72**: 041711.
5. Dudok T H, Krupych O M, Savaryn V I, Cherpak V V, Fechan A V, Gudeika D, Grazulevicius J V, Pansu B and Nastishin Yu A, 2014. Lasing in a cholesteric liquid crystal doped with derivative of triphenylamine and 1,8-naphthalimide, and optical characterization of the materials. *Ukr. J. Phys. Opt.* **15**: 162–172.
6. Varin C and Piche M, 2002. Acceleration of ultra-relativistic electrons using high-intensity TM01 laser beams. *Appl. Phys. B*. **74**: S83–S88.
7. Kozawa Y and Sato S, 2005. Generation of a radially polarized laser beam by use of a conical Brewster prism. *Opt. Lett.* **30**: 3063–3065.
8. Li J L, Ueda K, Musha M, Shirakawa A and Zhang Z M, 2007. Converging-axicon-based radially polarized ytterbium fiber laser and evidence on the mode profile inside the gain fiber. *Opt. Lett.* **32**: 1360–1362.
9. Toussaint K C, Park S, Jureller J E and Scherer N F, 2005. Generation of optical vector beams with a diffractive optical element interferometer. *Opt. Lett.* **30**: 2846–2848.
10. Churin E G, Hoßfeld J and Tschudi T, 1993. Polarization configurations with singular point formed by computer-generated holograms. *Opt. Commun.* **99**: 13–17.
11. Bomzon Z, Biener G, Kleiner V and Hasman E, 2002. Radially and azimuthally polarized beams generated by space-variant dielectric subwavelength gratings. *Opt. Lett.* **27**: 285–287.

12. Moh K J, Yuan X-C, Bu J, Low D K Y and Burge R E, 2006. Direct noninterference cylindrical vector beam generation applied in the femtosecond regime. *Appl. Phys. Lett.* **89**: 251114.
13. Xi-Lin Wang, Jianping Ding, Wei-Jiang Ni, Cheng-Shan Guo and Hui-Tian Wang, 2007. Generation of arbitrary vector beams with a spatial light modulator and a common path interferometric arrangement. *Opt. Lett.* **32**: 3549–3551.
14. Kleman M and Lavrentovich O D. *Soft Matter Physics. An Introduction*. Berlin Heidelberg New York Tokyo: Springer (2003).
15. Lavrentovich O D and Nastishin Yu A, 1987. Defects with nontrivial topological charges in hybrid-aligned films of nematic liquid crystal. *Sov. Phys.: Crystallogr.* **34**: 914–917.
16. Lavrentovich O D and Nastishin Yu A, 1990. Defects in degenerate hybrid aligned nematic liquid crystals. *Europhys. Lett.* **13**: 135–141.
17. Voloschenko D and Lavrentovich O D, 2000. Optical vortices generated by dislocations in a cholesteric liquid crystal. *Opt. Lett.* **25**: 317–319.
18. Nastishin Yu A, Meyer C and Kleman M, 2008. Imperfect focal conic domains in A smectics: a textural analysis. *Liq. Cryst.* **35**: 609–624.
19. Kleman M, Lavrentovich O D and Nastishin Yu A. Dislocations and disclinations in mesomorphic phases. In: *Dislocations in Solids*, vol. 12, Ed. by F R N Nabarro and J P Hirth, Elsevier (2004), pp. 147–271.

Nastishin Yu. A., Dudok T., Savaryn V., Kostyrko M., Vasylykiv Yu., Hrabchak V., Ryzhov Ye. and Vlokh R. 2021. Liquid crystal textures and optical characterization of a dye-doped nematic for generating vector beams. *Ukr.J.Phys.Opt.* **22**: 151 – 164. doi: 10.3116/16091833/22/3/151/2021

Анотація. У цій роботі розглянуто рідкокристалічні (РК) текстури з неоднорідними конфігураціями просторового поля директора та азимутальними сингулярностями з точки зору їхнього застосування для генерації векторних та скалярних оптичних вихрових пучків. Щоб сформувати композитний векторний пучок, РК-зразок повинен бути світлопоглинаючим і дихроїчним. Для генерування скалярного вихрового пучка слід сформувати вилкоподібний дефект у РК-комірці. З метою кількісного оцінювання цих можливостей виконано оптичну характеристику нематика, легованого барвником. А саме, нами використано відомі методи характеристики для вимірювання звичайного та незвичайного показників поглинання світла, лінійного дихроїзму, дисперсії приросту лінійного двозаломлення та скалярного параметра орієнтаційного порядку. Оскільки світлопоглинальна добавка, використана нами, є флуоресцентним барвником, то векторні пучки можна одержати і в пройденому світлі, і в світлі флуоресценції. З цієї причини виміряно також флуоресценцію досліджуваного нами нематика, легованого барвником.